

Physical and antibacterial properties of polyvinyl alcohol films reinforced with quaternized cellulose

Dongying Hu, Lijuan Wang

Key Laboratory of Bio-based Material Science and Technology of Ministry of Education, Northeast Forestry University, 26 Hexing Road, Harbin 150040, China

Correspondence to: Lijuan Wang (E-mail: donglinwlj@163.com)

ABSTRACT: Hydroxypropyltrimethylammonium chloride cellulose (CM) was homogeneously synthesized in a NaOH/urea aqueous solution. CM was blended in a polyvinyl alcohol (PVA) matrix to produce composite films via co-regeneration from the alkaline solution. The PVA film and the blend films were characterized by Fourier transform infrared spectroscopy, X-ray diffraction measurements and scanning electron microscopy. The mechanical properties, water swelling ratio, hydrophobicity, light transmission, and antibacterial activity against *Staphylococcus aureus* and *Escherichia coli* were also evaluated. The results showed that CM could interact with PVA by hydrogen bonding and exhibit an obvious reinforcement effect. The addition of CM improved the surface roughness, hydrophobicity and water swelling ratio, especially, the antibacterial activity. However, compared with neat PVA film, the elasticity and optical transmission decreased. The increased tensile strength, powerful antibacterial activity, and medium light transmission indicate that the biocompatible blend film will become an exceptional alternative in functional bio-material field. © 2016 Wiley Periodicals, Inc. *J. Appl. Polym. Sci.* **2016**, *133*, 43552.

KEYWORDS: bio-materials; films; functionalization of polymers; packaging; properties and characterization

Received 9 December 2015; accepted 18 February 2016

DOI: 10.1002/app.43552

INTRODUCTION

Chemically synthesized polymeric plastic films are common and widely used for food packaging because of their good properties, ease of processing and low cost.¹ However, such packaging material is hard to be degraded, causing a number of environmental problems.² So, biodegradable materials have attracted an increasing amount of attention due to the growing concerns on the environmental problem resulting from non-biodegradable materials especially in the area of food packing.³ Polyvinyl alcohol (PVA) is among the most commonly used synthetic polymers because of its favorable properties such as nontoxicity, biocompatibility, and film-forming ability.⁴ It is an environmentally friendly polymer easily biodegraded by adapted microorganisms into CO₂ and water.⁵ Despite the high hydrophilicity makes it very sensitive to moisture attack. Otherwise, the absence of antibacterial properties makes it unable to provide a barrier against bacteria. The improvement of antimicrobial properties of PVA films is a key to further expand its application areas. One interesting approach involved in the combination with other biopolymers to obtain composite film with special functions and improved properties.

The addition of antimicrobial compounds into films can effectively inhibit or delay the growth of microorganisms that may be

present on the surface of food products, which is safer in contrast to direct application of the antimicrobial agents on the surface of food system.^{6,7} In previous works, some antibacterial compounds including antibiotics, halogens and inorganic nanoparticles (Ag, Hg, ZnO, CuO, TiO₂)^{8–11} were directly incorporated into the packaging materials. However, the toxic substance will go into the environment from the waste film and cause serious secondary pollution. So, all antibacterial systems need to combine with other characteristics, such as environmental friendly, low toxicity or non-toxicity, cost efficiency and easy incorporation.

Cellulose is the most abundant renewable natural biopolymers on earth and has become an attractive alternative for the preparation of environment-friendly and biocompatible materials with other biopolymers.^{12–15} Chemical modification of cellulose is an effective approach for preparing cellulose derivatives with special properties. Quaternary ammonium compound is the most widely used antimicrobial agents due to their antibacterial properties, low toxicity and environmental compatibility.¹⁶ Quaternary ammonium groups can be grafted onto the cellulose molecules through the reaction with the C₆ primary hydroxyl groups of cellulose, endowing cellulose with antibacterial properties. Furthermore, the chemical structure of PVA favors the formation of interaction with hydroxyl groups of the natural

polymers, such as chitosan, sodium alginate, xylan and gelatin,^{17–19} resulting in the higher physical properties of PVA films. Therefore, it is also a good strategy for blending functionalized cellulose with PVA to prepare composite film. Many researches about blend films of PVA and cellulose at different states have been carried out.^{20–22} However, the antibacterial PVA-based film incorporating quaternary ammonium group modified cellulose has not been previously investigated.

In the present work, microcrystalline cellulose (MCC) was grafted with 3-chloro-2-hydroxypropyltrimethylammonium chloride (CHPTAC) for preparing quarternized cellulose in NaOH/urea aqueous solution. The modified MCC was blended in PVA film to improve the antibacterial activity. The physical properties and structure between PVA and functionalized cellulose were studied by means of Fourier transfer infrared (FTIR) spectroscopy, X-ray diffraction (XRD) measurements, scanning electron microscopy (SEM), swelling analysis, tensile tests, and light-transmission measurements. Furthermore, the antimicrobial activity of the bio-composite films against Gram-negative (*Escherichia coli*) and Gram-positive (*Staphylococcus aureus*) bacteria was evaluated.

EXPERIMENTAL

Materials

MCC (Comprecel M101; degree of polymerization (DP) = 200), was purchased from Shanghai Shenmei Pharmaceutical Technology Co., Ltd. (Shanghai, China). PVA (average molecular weight (Mw) = 84000–89000 g/mol; DP = 1700–1800; 88% alcoholysis) was purchased from Sinopec Shanghai Petrochemical Co., Ltd. (Shanghai, China). 3-Chloro-2-hydroxypropyltrimethylammonium chloride (CHPTAC) was purchased from Guofeng Fine Chemical Co., Ltd. (Shandong, China). All other chemicals were of analytical grade and were used as received without further purification. The microorganisms used in this study namely *Escherichia coli* (*E. coli*) and *Staphylococcus aureus* (*S. aureus*), were provided by Qingdao Hope Bio-Technology Co., Ltd. (Qingdao, China). All other biochemical reagents were purchased from AoBoXing Bio-tech Co., Ltd. (Beijing, China).

Sample Preparation

Preparation of CM. According to a previous work,^{23,24} a NaOH/urea aqueous solution was prepared by mixing 7 wt % NaOH, 12 wt % urea and distilled water. 2 g of MCC was dispersed into a NaOH/urea solution, which was then cooled to -12.5°C . The frozen mixture was then thawed and vigorously stirred for 5 min and a transparent cellulose solution with concentration of 2 wt % was obtained. Subsequently, a certain amount of CHPTAC was added into the cellulose solution, and the mixture was stirred at 25°C for 24 h. In the mixture, the mole ratio of CHPTAC to the anhydroglucose unit in the cellulose molecules was 6:1. The obtained functionalized MCC derivative solution was separated into two parts. One was neutralized with HCl solution, dialyzed, and freeze-dried to obtain the purified functionalized MCC according to the method²⁵ for further analysis, coded as CM. The other was stored at 0°C for direct use in the preparation of PVA/CM composite film.

Preparation of PVA/CM Composite Film. PVA was dissolved in deionized water under constant stirring at 80°C for 2 h to

achieve a solution of 8.80 wt %. PVA and CM solutions were mixed together, and the resulting solution was stirred vigorously for 30 min. After the solution was degassed in a vacuum oven, it was transferred into a glass mold ($30\text{ cm} \times 30\text{ cm} \times 5\text{ cm}$), then, it was immersed in a 1000 mL of 5 wt % $\text{CaCl}_2/3\text{ wt \% HCl}/92\text{ wt \% H}_2\text{O}$ aqueous solution for 10 min at 25°C to obtain regenerated PVA/CM film with uniform thickness. The resulted composite films were washed with deionized water and then the wet films were then fixed onto a polyvinyl chloride (PVC) sheet to prevent shrinkage, and finally dried in air at 25°C . The PVA/CM films were denoted as CMP-5, CMP-10, CMP-15 and CMP-20 in a weight proportion of 95:5; 90:10; 85:15 and 80:20, respectively. The control (PVA film) was obtained through the process as above but without addition of CM solution.

Characterization

Fourier Transforms Infrared (FTIR) Spectroscopy. FTIR spectra were obtained using a Thermo Nicolette 6700 spectrophotometer (Thermo Fisher Scientific Co., Ltd., MA) with attenuated total reflection (ATR) mode at a resolution of 4 cm^{-1} .

X-ray Diffraction Patterns (XRD). XRD patterns of the samples were carried out using a D/max-2200 diffractometer (Rigaku, Japan) at a scanning rate of $5^{\circ}/\text{min}$. The diffraction patterns were recorded from 5° to 40° using Cu-K α radiation at 40 kV and 30 mA.

Elemental Analysis. The nitrogen content (N %) of CM was measured on an elemental analyzer (EA 3000, Arvator, Italy).

X-ray Photoelectron Spectroscopy (XPS). The valence state of nitrogen in the composite films was determined by using a K-Alpha XPS analyzer (Thermo Fisher Scientific Company, USA).

Morphology of the Films. The upper surface and the cross-section morphology of the films were examined using a Quanta 200 scanning electron microscope (Philips-FEI Co., AMS, Netherlands) after coated with gold. The accelerating voltage was 20 kv.

Mechanical Properties of the Films. The thicknesses of the films were measured with an ID-C112XBS micrometer (Mitutoyo Corp., Tokyo, Japan), and reported as the average from ten random points. Tensile tests of the membranes were carried out using an auto tensile tester (XLW-PC, PARAM, Jinan, China) equipment with a 500 N load cell. Measurements were performed with a strain rate of 300 mm/min. The samples had widths and lengths of 10 and 150 mm, respectively. Five specimens of each sample were tested.

The Light Transmission Measurements. The light transmittance spectra of the composite films were measured in the wave length ranging from 200 to 800 nm using an ultraviolet-visible (UV-vis) spectrophotometer (UV-2600, Shimadzu, Kyoto, Japan).

Swelling Studies. The water absorption capacity of the films was determined by measuring the initial weight of the dry films, and subsequently after they were immersed into distilled water at 37°C . Before measuring the weight of the swollen films, the extra surface water of the wet films was removed by filter paper. The percentage swelling was calculated as follows:

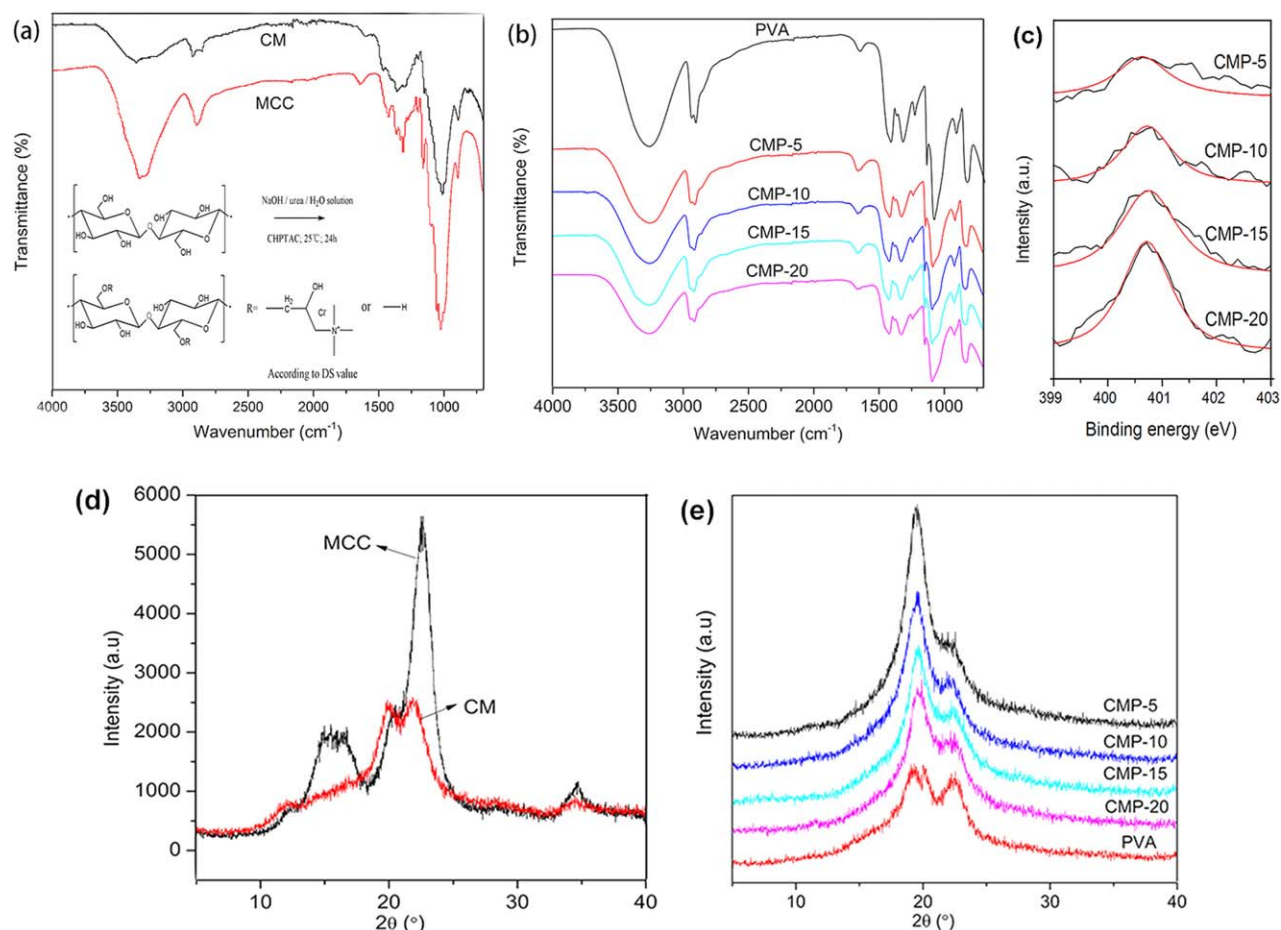


Figure 1. FTIR spectra of (a) MCC, quaternized MCC (CM), and (b) PVA, CMP-5, CMP-10, CMP-15, and CMP-20 films. (c) N1s XPS spectra of YMP films. (d) XRD patterns of MCC, quaternized MCC (CM), and (e) PVA, CMP-5, CMP-10, CMP-15, and CMP-20 films. [Color figure can be viewed in the online issue, which is available at wileyonlinelibrary.com.]

$$\% \text{ Swelling} = (W_s - W_d) / W_d \times 100$$

Where W_s denotes the weight of the swollen films after required period of time, and W_d is the initial dry weight of the films.

Water Contact Angle (CA) Measurement. CA measurements of 5 μL water droplets on the film surface were measured at 23 $^{\circ}\text{C}$ using an optical contact angle meter (Powreach, JC2000C, China).

Antimicrobial Properties. Antimicrobial activities of the films were determined against gram-negative bacteria (*E. coli*) and gram-positive bacteria (*S. aureus*) by measuring the inhibition zone around each film disc. 0.1 mL of bacteria suspensions (10^8 CFU/mL) of *E. coli* or *S. aureus* were distributed into the nutrient agar (NA) agar medium. The films were cut into circular discs 8 mm in diameter, and then were placed on the medium previously inoculated with the test bacteria. Each agar plate was kept for incubation at 37 $^{\circ}\text{C}$ for 24 h, then the inhibition zones of the tested film were measured. Three replicate tests were carried out under the same conditions for each sample.

The Japanese industrial standard JIS Z 2801:2010 is a common method for assessing the antimicrobial efficacy of materials. So, the antibacterial efficacy of the CMP films was also evaluated by

the standard. A pure PVA film was used as a control sample. 0.1 mL of bacteria suspensions (2.0×10^5 CFU/mL) of *E. coli* or *S. aureus* were inoculated onto the samples and cultured at 37 $^{\circ}\text{C}$ for 24 h. Subsequently, the number of viable bacterial was counted. The value of antimicrobial efficacy (R) was calculated to evaluate the biocide character of surface. Three replicate tests were performed under the same conditions for each sample.

Statistical Analysis. Multiple samples were tested, and data were reported are average values \pm standard deviations (SD). The data were analyzed by one way analysis of variance (ANOVA) through the SPSS software and differences among mean values were processed by the Duncan's multiple-range tests. Significance was defined at P values of < 0.05 .

RESULTS AND DISCUSSION

FTIR Spectroscopy

The structural changes were studied using FTIR spectroscopy. As shown in Figure 1(a), bands for CM appeared at 3353 cm^{-1} (O—H stretching), at 2923 and 2852 cm^{-1} [$\nu_{\text{as}}(\text{CH}_2)$, $\nu_{\text{s}}(\text{CH}_2)$], as well as at 1470 cm^{-1} (C—N), 1312 , 1113 , 1019 and 899 cm^{-1} (glucopyranose ring), which indicate that quaternary ammonium group was successfully grafted onto the MCC skeleton.²⁶ Moreover, the degree of substitution of CM is 0.42 obtained from

elemental analysis, which further supports the above results. Figure 1(b) shows the FTIR spectra of PVA and CMP films. Characteristic bands of PVA were observed at 3283 cm^{-1} (O—H stretching), 2913 cm^{-1} (C—H bending), 1732 cm^{-1} (C=O stretching), and 1086 cm^{-1} (C—O stretching).²⁷ In case of CMP composite films, characteristic bands of PVA are apparent; however, characteristic bands of CM almost overlap. As shown in Figure 1(c), the peak at $\sim 400.75\text{ eV}$ in the XPS spectra is consistent with nitrogen in quaternary ammonium groups,²⁸ which further confirms the introduction of CM into the blend films. Moreover, the O—H stretching vibration bands of the CMP blend films at $3260\text{--}3240\text{ cm}^{-1}$ broadened and shifted to a lower wavenumber, indicating the strong intermolecular hydrogen bonding between CM and PVA in the films. The interaction will favor the tensile strength of the blend film.

XRD Analysis

The XRD patterns of MCC and CM are presented in Figure 1(d). The characteristic peaks of MCC are located at 2θ values of 14.9° , 16.4° , 22.6° and 34.6° , which are typical diffraction of cellulose I angles. However, besides, weaker characteristic peaks of cellulose I, the pattern of CM showed a broad peak at 2θ values of 12.3° , 20.1° , which characterized for the crystalline form of cellulose II. These results indicated that a partial crystal transition from cellulose I to cellulose II during the dissolution, modification and subsequent regeneration processes. So, mixed crystals of cellulose I and cellulose II occurred in CM. The patterns of the PVA film and PVA-based blend films with different amount of CM are shown in Figure 1(e). The peaks at 2θ values of 19.5° and 22.4° are characteristics of the structure of crystalline PVA. The intensities of the peaks of CMP films are all greater than those of pure PVA film. These results indicate that the intermolecular and intramolecular hydrogen bonds between PVA and CM were strong. Otherwise, the peaks become weaker with the increase of amount of CM in the blend films. The greater amounts of NaOH and urea, which came from the NaOH/urea aqueous solution during film preparation process, remained in the blend film as the CM content increased. The OH^- , C=O and &sbond;NH_2 groups could form hydrogen bonds with hydroxyl group in PVA and CM, which hindered the intramolecular interaction in PVA or CM and the intermolecular interaction between PVA and CM. Moreover, it is also due to the decreased dispersion at higher CM content.

SEM Images

Figure 2 shows the micrographs of the upper surface and cross section of PVA and CMP films. PVA film had a smooth surface, but its cross section images indicated the presence of zones with different morphology due to the coexistence of crystalline and amorphous regions in the film, as reported by Cano *et al.*²⁹ Compared with PVA film, the CMP films showed rougher surfaces, moreover, phase separation can be clearly observed on the cross section photographs when the proportion of CM in the blend increased from 5 wt % to 20 wt %. These observations indicate that incompatibility between PVA and CM became more obvious at higher CM content in the blend film. Overall, CM was miscible with PVA, and both formed a uniform film at low CM contents.

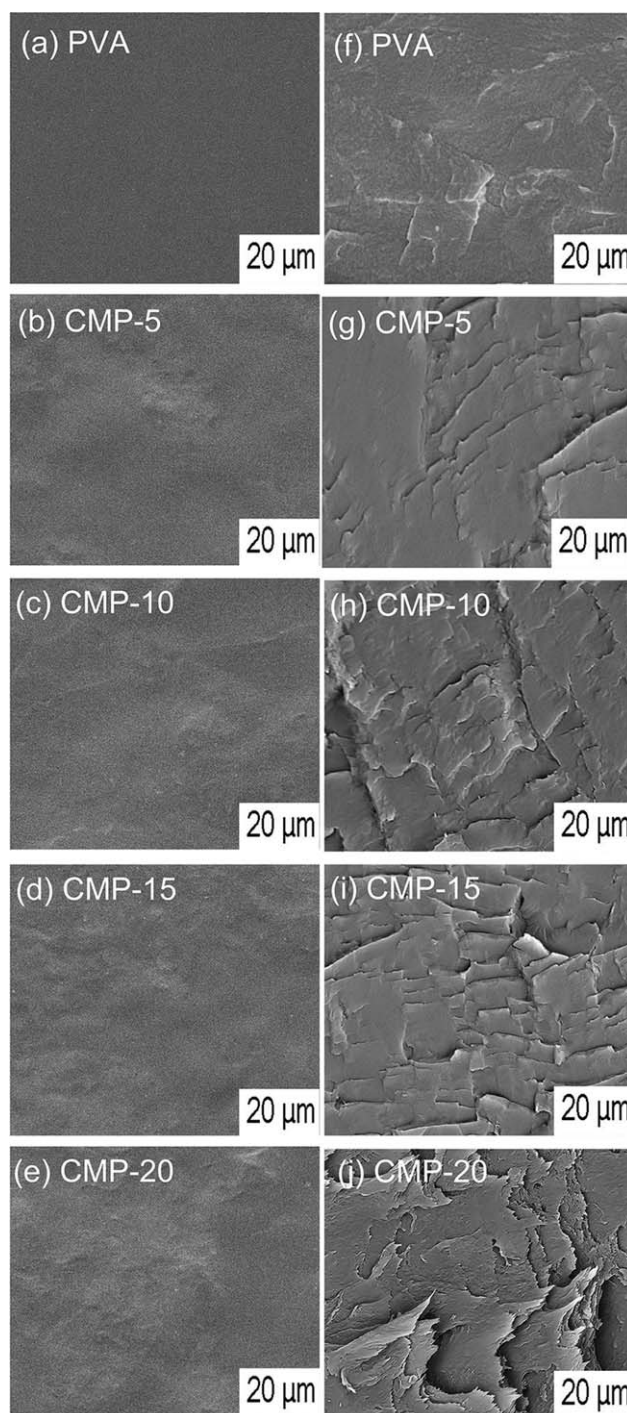


Figure 2. SEM micrographs of the upper surfaces (a–e) and cross sections (f–j) of the films (PVA, CMP-5, CMP-10, CMP-15 and CMP-20).

Mechanical Properties

The mechanical properties of pure PVA and PVA/CM blend films with 5, 10, 15, and 20 wt % CM are presented in Figure 3 ($P < 0.05$). The tensile strength and elongation at break of the PVA film are $28.83 \pm 1.04\text{ MPa}$ and $331.48 \pm 2.57\%$, respectively. Compared with PVA film, the addition of CM into PVA film has obvious effect on the mechanical properties of the films. The tensile strength and the elongation at break of the

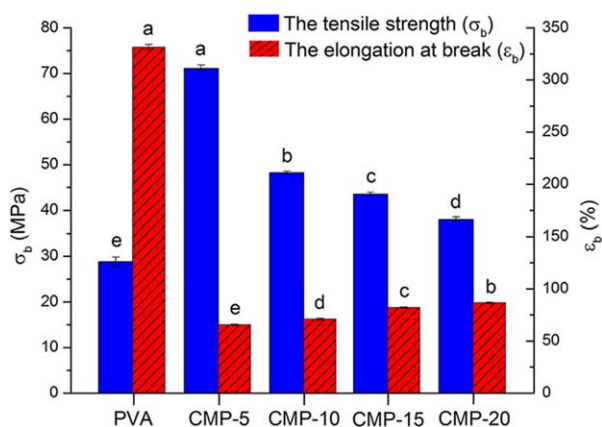


Figure 3. Mechanical properties of the PVA and CMP films. The data are representative of the results from five independent experiments and are expressed as the means \pm standard deviation. Different letters indicate significantly different films determined by Duncan's multiple-range tests ($P < 0.05$). [Color figure can be viewed in the online issue, which is available at wileyonlinelibrary.com.]

resulted film reached the maximum value of 71.14 ± 0.73 MPa and the minimum value of $65.56 \pm 0.48\%$, when 5 wt % of CM was added. This result implies that a strong interaction between PVA and CM molecules and exceptional reinforcement of the PVA matrix with the addition of the CM. For CM content higher than 5 wt %, the tensile strength decreased and the elongation at break increased because of the decreased CM dispersion, making the tensile failure easily occur. Furthermore, as a plasticizer, more residual urea in the blend film from the regeneration process can cause the decreased tensile strength and increased elongation at break.³⁰

The Swelling Ratio, and Water Contact Angle (WCA) of the Films

The swelling behavior of films is an important property for their practical applications. Figure 4 displays the effect of different CM

contents on water solution uptake percentages of bio-composite films with time ($P < 0.05$). The swelling ratio increases with time and after 18 h it gets leveled off. All the CMP films exhibited high swelling ratios at the range from 198.11 to 344.82%, and more, the swelling ratios was increased by the increasing of the CM contents. The high swelling ratios should be attributed to the good hydratability of CM with large amounts of quaternary ammonium salt groups.³¹

The surface wettability of films was usually tested by measuring the water contact angle (WCA) ($P < 0.05$). As shown in Figure 4, the results reveal that the use of CM led to a reduction in hydrophilicity of the CMP films compared to the PVA film. The WCA of PVA film was founded to be $44 \pm 1.5^\circ$. In contrast, the WCA values for CMP films (CMP-5, CMP-10, CMP-15, CMP-20) are $59 \pm 2.5^\circ$, $65 \pm 1.26^\circ$, $68 \pm 2.25^\circ$, $77 \pm 1.76^\circ$, respectively. The strong interaction between CM and PVA resulted in the hydrophilicity reduce of the film surface.³² In addition, the hydrophobicity largely depended on surface roughness of CMP films increased with the higher CM content, which was corroborated by the SEM images.

The Optical Transmittance Analysis

The optical transmittance (T_r) is a useful criterion for the compatibility of the composite element, and also related to the structure of the materials.³³ Figure 5 shows the UV-vis spectra of pure PVA and CMP films with $64 \pm 8 \mu\text{m}$ thickness and the photographs of the flower before and after covered with the films. PVA is a transparent polymer and the transmittance of PVA film reached about 90% at 400~800 nm wavelength. We can clearly see the similar flower before and after covered with PVA film. In contrast, the transmittances of CMP films were decreased with the addition of CM. When the CM content was 5, 10, and 15 wt %, the transmittance (600 nm) was 76%, 74%, and 70%, respectively. The transmittance significantly decreased to around 60% as the CM content increased to 20 wt %. The

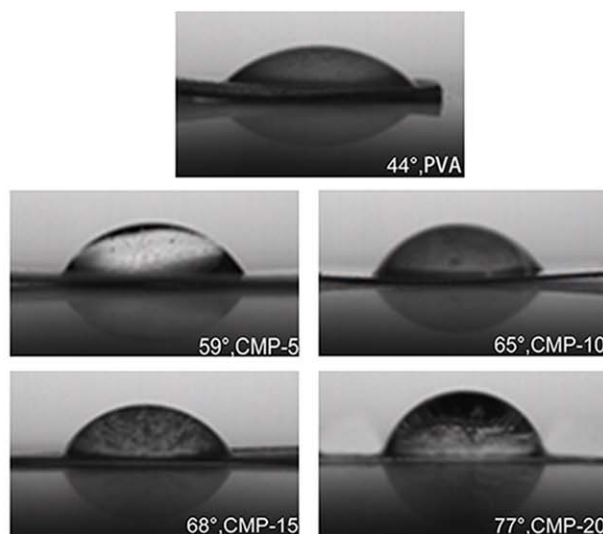
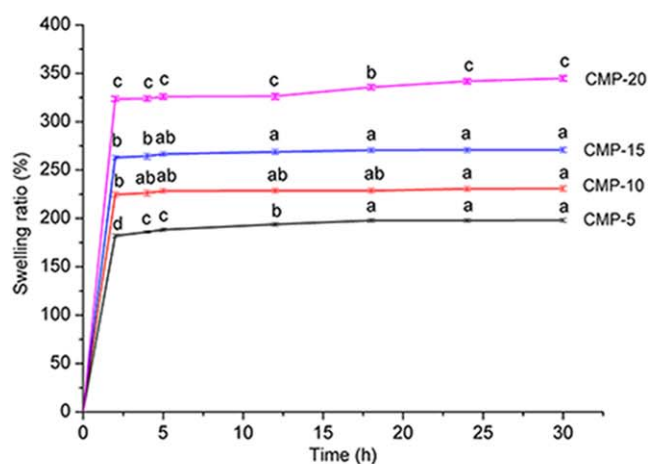


Figure 4. Swelling properties of bio-composite films (CMP-5, CMP-10, CMP-15, CMP-20) and WCA on upper surface for films of PVA, CMP-5, CMP-10, CMP-15, CMP-20 with 5s. The data are representative of the results from three independent experiments and are expressed as the means \pm standard deviation. Different letters indicate significantly different time determined by Duncan's multiple-range tests ($P < 0.05$). [Color figure can be viewed in the online issue, which is available at wileyonlinelibrary.com.]

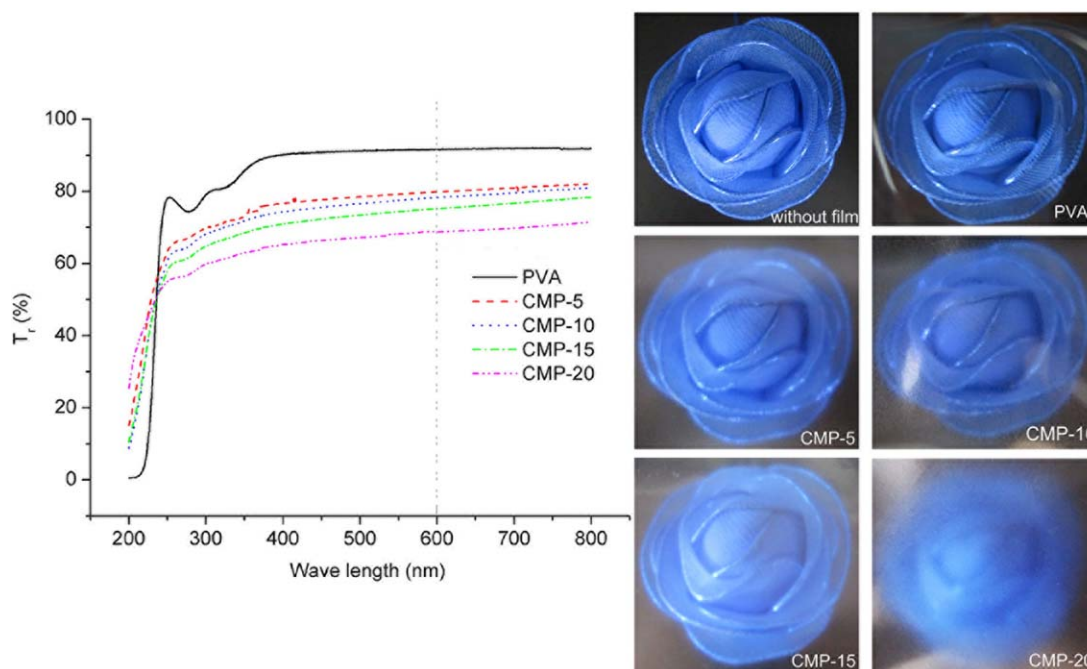


Figure 5. The films of optical transmittance curves and photographs (PVA, CMP-5, CMP-10, CMP-15, CMP-20). [Color figure can be viewed in the online issue, which is available at wileyonlinelibrary.com.]

blend films became more opaque and the photo of the covered flower became more blurry with the increase of CM content. This may be due to the decreased dispersion and to the compatibility at higher CM content. These in turn increase the number of interfaces in the blend films, leading to optical scattering and refraction. Therefore, the transmission light decreased. In fact, the optical properties are very important for packaging films because of a transparent film is feasible for viewing the packed product. Otherwise, opaque film is also favorable for reducing deteriorations catalyzed by light.

Antibacterial Properties

The antibacterial activity of the composite films was determined by measuring the diameter of the inhibition zone. Figure 6 shows the effects of the films against Gram-positive (*S. aureus*) and Gram-negative (*E. coli*) bacteria ($P < 0.05$). The results showed

that there was no clear inhibitory zone surrounding PVA film disc, suggesting that pure PVA had no antibacterial activity. In contrast, the inhibitory zone diameters of CMP-5, CMP-10, CMP-15, and CMP-20 films are 16.0, 18.8, 22.4, 27.3 mm and 18.1, 29.2, 22.0, 37.2 mm for *S. aureus* and *E. coli*, respectively. These results indicate that the CMP films had an obvious antibacterial effect against both the tested bacteria because of the antibacterial activity of the ammonium group. The antibacterial mechanism is believed that the positive charge of the quaternized group can be absorbed onto the negatively charged cell surface of bacteria, making the structure of the outer membrane changed and cytoplasmic constituents released, ultimately resulting in bacterial death.³⁴ The antibacterial activity of the CMP film was significantly improved as the CM content increased from 5 to 20 wt % because of the presence of more ammonium groups in the blend film. Otherwise, the activity of the blend films against

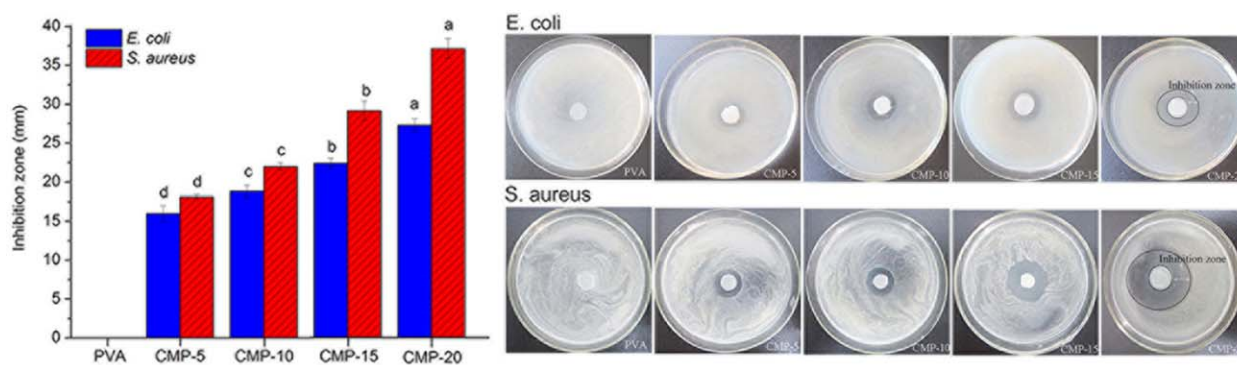


Figure 6. The antibacterial activity of the films against *E. coli* and *S. aureus*. The data are representative of the results from three independent experiments and are expressed as the means \pm standard deviation. Different letters indicate significantly different films determined by Duncan's multiple-range tests ($P < 0.05$). [Color figure can be viewed in the online issue, which is available at wileyonlinelibrary.com.]

Table I. The Values of Antimicrobial Efficacy (*R*) of the Blend Films

	<i>E. coli</i>	<i>S. aureus</i>
CMP-5	3.55 ± 0.02d	3.72 ± 0.02c
CMP-10	3.69 ± 0.03c	3.82 ± 0.04c
CMP-15	3.79 ± 0.04b	4.28 ± 0.12b
CMP-20	4.22 ± 0.09a	5.10 ± 0.50a

Values are expressed as mean ± standard deviation. Different letters in the same column indicate significant differences ($P < 0.05$).

S. aureus was stronger than against *E. Coli*. The reason of the difference in antibacterial activity is that *S. aureus* is more susceptible to sanitizers than *E. Coli* because the latter has a relatively impermeable lipid-based outer membrane.³⁵ The results indicate that the antibacterial efficacy of the blend film can be controlled by the amount of CM added. Moreover, the values of antimicrobial efficacy (*R*) were obtained according to JIS Z 2801:2010 standard as shown in Table I. The value of $R > 2$ represents a good antimicrobial activity of antimicrobial products and can be applicable subject to the agreement between parties concerned with delivery.³⁶ For CMP films, the high average *R* values (> 2) were consistent with the results from the inhibition zone test, which further quantified the antimicrobial capability of the blend films incorporated with CM.

CONCLUSIONS

In this work, hydroxypropyltrimethylammonium chloride cellulose (CM) was successfully synthesized in NaOH/urea aqueous system by grafting 3-chloro-2-hydroxypropyltriethylammonium groups onto cellulose skeleton. The PVA-based composite films incorporating CM were prepared through regeneration from the NaOH/urea aqueous solutions. CM is miscible with PVA and form uniform film under low CM content. Compared with neat PVA film, the addition of CM improved the surface roughness, hydrophobicity, and water swelling ratio of the films, and endowed the films with strong antibacterial activity, however, the elasticity and optical transmission was decreased. This study provided a feasible and easy method to produce PVA-based blend films containing modified cellulose. The resulted biocompatible blend films with powerful antibacterial activity will exhibit a promising application in many fields.

ACKNOWLEDGMENTS

This work was supported by the National Natural Science Foundation of China (31470612).

REFERENCES

- Debiagi, F.; Kobayashi, R. K. T.; Nakazato, G.; Panagio, L. A.; Mali, S. *Ind. Crop. Prod.* **2014**, *52*, 664.
- Ghanbarzadeh, B.; Almasi, H.; Entezami, A. A. *Ind. Crop. Prod.* **2011**, *33*, 229.
- Bocchini, S.; Battagazzore, D.; Frache, A. *Carbohydr. Polym.* **2010**, *82*, 802.
- Gupta, B.; Agarwal, R.; Sarwar Alam, M. *J. Appl. Polym. Sci.* **2013**, *127*, 1301.
- Peresin, M. S.; Habibi, Y.; Vesterinen, A. H.; Rojas, O. J.; Pawlak, J. J.; Seppala, J. V. *Biomacromolecules* **2010**, *11*, 2471.
- Atef, M.; Rezaei, M.; Behrooz, R. *Food Hydrocolloids* **2015**, *45*, 150.
- Muppalla, S. R.; Kanatt, S. R.; Chawla, S. P.; Sharma, A. *Food Packag. Shelf Life* **2014**, *2*, 51.
- Andresen, M.; Stenstad, P.; Moretro, T.; Langsrud, S.; Syverud, K.; Johansson, L. S.; Stenius, P. *Biomacromolecules* **2007**, *8*, 2149.
- De Moura, M. R.; Mattoso, L. H. C.; Zucolotto, V. J. *Food Eng.* **2012**, *109*, 520.
- Espitia, P. J.; Soares Nde, F.; Teofilo, R. F.; Coimbra, J. S.; Vitor, D. M.; Batista, R. A.; Ferreira, S. O.; de Andrade, N. J.; Medeiros, E. A. *Carbohydr. Polym.* **2013**, *94*, 199.
- Shankar, S.; Teng, X. N.; Li, G. B.; Rhim, J. W. *Food Hydrocolloids* **2015**, *45*, 264.
- Almeida, E. V. R.; Frollini, E.; Castellan, A.; Coma, V. *Carbohydr. Polym.* **2010**, *80*, 655.
- De Silva, R.; Vongsanga, K.; Wang, X.; Byrne, N. *Carbohydr. Polym.* **2015**, *121*, 382.
- Lavoine, N.; Desloges, I.; Dufresne, A.; Bras, J. *Carbohydr. Polym.* **2012**, *90*, 735.
- Pang, J.; Wu, M.; Zhang, Q.; Tan, X.; Xu, F.; Zhang, X.; Sun, R. *Carbohydr. Polym.* **2015**, *121*, 71.
- Xu, W. Z.; Gao, G.; Kadla, J. F. *Cellulose* **2013**, *20*, 1187.
- Pereira, V. A.; de Arruda, I. N. Q.; Stefani, R. *Food Hydrocolloids* **2015**, *43*, 180.
- Sirvio, J. A.; Kolehmainen, A.; Liimatainen, H.; Niinimäki, J.; Hormi, O. E. *Food Chem.* **2014**, *151*, 343.
- Zu, Y.; Zhang, Y.; Zhao, X.; Shan, C.; Zu, S.; Wang, K.; Li, Y.; Ge, Y. *Int. J. Biol. Macromol.* **2012**, *50*, 82.
- Cha, R. T.; Wang, C. Y.; Cheng, S. L.; He, Z. B.; Jiang, X. Y. *Carbohydr. Polym.* **2014**, *110*, 298.
- Pereira, A. L.; do Nascimento, D. M.; Souza Filho Mde, S.; Morais, J. P.; Vasconcelos, N. F.; Feitosa, J. P.; Brigida, A. I.; Rosa Mde, F. *Carbohydr. Polym.* **2014**, *112*, 165.
- Xu, X.; Yang, Y. Q.; Xing, Y. Y.; Yang, J. F.; Wang, S. F. *Carbohydr. Polym.* **2013**, *98*, 1573.
- Aulin, C.; Karabulut, E.; Tran, A.; Wagberg, L.; Lindstrom, T. *ACS Appl. Mater. Interfaces* **2013**, *5*, 7352.
- Song, Y. B.; Sun, Y. X.; Zhang, X. Z.; Zhou, J. P.; Zhang, L. N. *Biomacromolecules* **2008**, *9*, 2259.
- Song, Y. B.; Zhang, J.; Gan, W. P.; Zhou, J. P.; Zhang, L. N. *Ind. Eng. Chem. Res.* **2010**, *49*, 1242.
- Adel, A. M.; El-Wahab, Z. H. A.; Ibrahim, A. A.; Al-Shemy, M. T. *Carbohydr. Polym.* **2010**, *83*, 676.
- Ashfaq, M.; Khan, S.; Verma, N. *Biochem. Eng. J.* **2014**, *90*, 79.
- Zhang, X.; Tan, J.; Wei, X.; Wang, L. *Carbohydr. Polym.* **2013**, *92*, 1497.

29. Cano, A.; Fortunati, E.; Cháfer, M.; Kenny, J. M.; Chiralt, A.; González-Martínez, C. *Food Hydrocolloids* **2015**, *48*, 84.
30. Ma, X. F.; Yu, J. G.; Wan, J. J. *Carbohydr. Polym.* **2006**, *64*, 267.
31. Yu, Q. A.; Song, Y. N.; Shi, X. M.; Xu, C. Y.; Bin, Y. Z. *Carbohydr. Polym.* **2011**, *84*, 465.
32. Huang, D. J.; Wang, W. B.; Xu, J. X.; Wang, A. Q. *Chem. Eng. J.* **2012**, *210*, 166.
33. Yang, Q. L.; Lue, A.; Zhang, L. N. *Compos. Sci. Technol.* **2010**, *70*, 2319.
34. Fan, L. H.; Cao, M.; Gao, S.; Wang, W. P.; Peng, K.; Tan, C.; Wen, F.; Tao, S. X.; Xie, W. G. *Carbohydr. Polym.* **2012**, *88*, 707.
35. Shariatnia, Z.; Fazli, M. *Food Hydrocolloids* **2015**, *46*, 112.
36. Osés, J.; Palacio, J. F.; Kulkarni, S.; Medrano, A.; García, J. A.; Rodríguez, R. *Appl. Surf. Sci.* **2014**, *310*, 56.